ELSEVIER

Journal of Structural Geology 27 (2005) 459–473

JOURNAL OF STRUCTURAL GEOLOGY

www.elsevier.com/locate/jsg

Sandbox models of relay ramp structure and evolution

R. Hus[a,*], V. Acocella[b], R. Funiciello[b], M. De Batist[a]

[a]*Renard Centre of Marine Geology (RCMG), University of Gent, B-9000 Gent, Belgium*
[b]*Dip. Scienze Geologiche Roma Tre, Largo S. L. Murialdo, 1—00146—Roma, Italy*

Received 17 February 2004; received in revised form 1 July 2004; accepted 9 September 2004
Available online 7 January 2005

Abstract

Relay ramps are a common feature formed during the growth of normal fault systems. We performed analogue experiments to investigate the structure and evolution of relay ramps. An extending rubber sheet induces extension at the base of a sand pack (brittle crust analogue). Silicone bars between the rubber and the sand control the location of fault nucleation. We tested the role of fault spacing, fault length, overlap length and fault strike in the evolution of relay ramps. The modelled relay ramps evolved in three stages, characterized by the growth of the normal faults, their interaction and linkage. Interaction and linkage occurred only when the combined length of the two interacting faults was larger than eight times their spacing. The length to width ratio of the relay ramps during the interaction stage showed preferred geometries, clustering around three. The propagation of the fault tips was observed both before and after the linkage stage. Overlap length and spacing relations of the modelled relay ramps are similar to those in nature, at different scales, and can be explained using existing mechanical models. Nevertheless, the further propagation of the fault tips after linkage has not been described previously.

Keywords: Sandbox models; Relay ramps; Normal fault systems; Fault linkage; Fault interaction

1. Introduction

Relay ramps are common in normal fault systems. They consist of an area of reoriented bedding between two normal faults that overlap in map view and have the same dip direction (Fig. 1; Peacock et al., 2000a). The reorientation or tilt of the bedding is the result of the decrease in displacement at the fault tips.

Numerous studies have described natural examples of relay ramps observed at different locations and scales (e.g. Macdonald, 1957; Larsen, 1988; Morley et al., 1990; Peacock, 1991; Peacock and Sanderson, 1991, 1994; Childs et al., 1995; Peacock et al., 2000b, amongst others). These studies highlight the role that relay ramps play in processes like the interaction and growth of faults, the evolution of drainage systems and the development of sedimentary basins (Peacock, 2002, and references therein). Moreover, relay ramps may influence the process of hydrocarbon migration and trapping (Morley et al., 1990; Peacock and Sanderson, 1994; Coskun, 1997).

The control of relay ramps on these different geological processes highlights the importance of defining their geometry and modes of evolution. The evolution of relay ramps is usually described in four different stages (Peacock and Sanderson, 1991, 1994). In stage 1, subparallel, stepping faults are isolated and do not interact. At stage 2, the relay ramp forms when the two faults start to overlap, causing a tilt of the bedding between them. Stage 3 marks the onset of fracturing inside the ramp and stage 4 is characterized by the connection of the two faults to form a composite fault. This model of relay ramp evolution has proven to be a good guide for the structural interpretation of relay ramps, even though dissimilarities have been reported between relay ramps at different scales (e.g. Peacock et al., 2000b).

Another approach for gaining insight into the evolution of relay ramps has been through mechanical modelling (Willemse et al., 1996; Willemse, 1997; Crider and Pollard, 1998). This modelling has permitted testing of the influence of several imposed parameters on the stress distribution

* Corresponding author. Tel.: +32-9-264-4637; fax; +32-9-264-4967
E-mail address: robert.hus@ugent.be (R. Hus).

0191-8141/$ - see front matter © 2005 Elsevier Ltd. All rights reserved.
doi:10.1016/j.jsg.2004.09.004

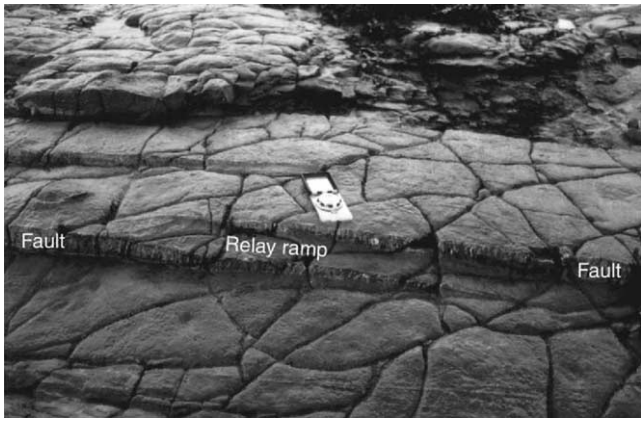

Fig. 1. Photograph of a small-scale relay ramp exposed on limestone bedding planes at East Quantoxhead, Somerset, UK. Bedding is tilted between two normal faults that overlap in map view. From Peacock (2002).

between overlapping normal fault segments that delimit relay ramps.

Several analogue experiments of extensional tectonics describe the occurrence of relay ramps (e.g. Childs et al., 1993; McClay and White, 1995; Clifton et al., 2000; Gupta and Scholz, 2000; Mansfield and Cartwright, 2001; McClay et al., 2002). Most of these experiments were aimed, however, at studying extensional processes in general and did not specifically consider the evolution of the relay ramps.

We performed a series of analogue experiments of relay ramps in normal fault systems, aimed at understanding their geometry and evolution. In our experiments, two fault segments were created, of which we were able to systematically vary the fault spacing, fault overlap length, segment length and the amount of finite extension. Our models differ from the previous experimental works because we have investigated how varying the initial configuration of two main faults affects the development and evolution of the overlap zone between them. The experimental results are discussed in the light of existing mechanical models and of known natural examples.

2. Experimental procedure

Scaled models should be geometrically, kinematically and dynamically similar to natural examples (Ramberg, 1981, and references therein). The density ratio between rocks and common experimental materials is $\rho^* \sim 0.5$, and the gravity ratio between model and nature is $g^* = 1$. Using a length ratio L^* between model and nature of $L^* = 10^{-5}$ (1 cm in our experiments corresponds to 1 km in nature), the corresponding stress ratio between model and nature becomes $\sigma^* = \rho^* g^* z^* \sim 5 \times 10^{-6}$. Cohesion c has the dimensions of stress; assuming a Mohr–Coulomb criterion and natural cohesion $c \sim 10^7$ Pa for the upper crustal rocks, a material with $c \sim 50$ Pa is required to simulate the brittle crust: for this purpose, dry quartz sand, with negligible cohesion, has been used. Dry quartz sand has been widely used as an analogue for the brittle behaviour of rocks in physical models (e.g. Horsfield, 1977; Dooley and McClay, 1997). Shear failure in brittle materials is practically independent of the strain rate (Mandl, 1988), therefore, the deformation rates of the models did not affect the evolution of the overlap zones. Nevertheless, to stay in the Newtonian flow regime of the silicone bars, the models were deformed with a low strain rate ($\sim 1.4 \times 10^{-4}$ m s^{-1}).

In experiments on thrust faulting, Faccenna et al. (1995) and Schreurs et al. (2001) used silicone putty bars at the base of the sand-pack, observing that the main faults propagated, within the sand, from the lateral interface between sand and putty. This technique has also been used recently to localise offset grabens (Le Calvez and Vendeville, 2002). We used the same technique in our experiments (Fig. 2a), placing two silicone bars at the base of the extending sand-pack. As a result, extension is focused at the sides of the silicone bars. We deformed our models with a velocity of 1.4×10^{-4} m s^{-1} in order to enhance the appropriate propagation of the deformation at the lateral interface between sand and silicone (Faccenna et al., 1995).

The use of the silicone bars at the base of the sand pack is purely restricted to controlling the location of the fault nucleation, and consequently the configuration (length, overlap length, spacing) of the overstepping normal faults (Fig. 2b). The silicone bars do not, therefore, correspond to any specific analogue in nature. The use of distinct silicone bars in our experiments allows us to avoid the use of a single, continuous basal moving plate, with a shaped velocity discontinuity, as used for example by Mauduit and Dauteuil (1996) and Acocella et al. (1999). In fact, when using rigid base plates consisting of two offset parallel segments, the part of the base plate that connects these segments also forms a (shaped) velocity discontinuity in the model. The presence of this discontinuity may significantly affect the geometry and kinematics of the resulting interaction zone.

Extension was achieved by means of a rubber sheet, located at the base of the sand pack (4–6 cm thick) and the silicone bars; the sheet was attached to a mobile (on one side) and a fixed (on the opposite side) wall (Fig. 2a). By moving the mobile plate away from the fixed one, the rubber sheet was stretched producing extension in the overlying sand pack.

In each model, opposed-dipping faults developed on both sides of the silicone bars, allowing us to study two relay zones during one run (Fig. 2a). The width of the silicone bars was usually 10 cm and the length and height varied between 7 and 25 cm and 1 and 2.5 cm, respectively. The width of the silicone bars was selected to prevent the interaction of these opposed-dipping faults. The sand thickness varied between 3.7 and 6 cm in the different experiments (Table 1).

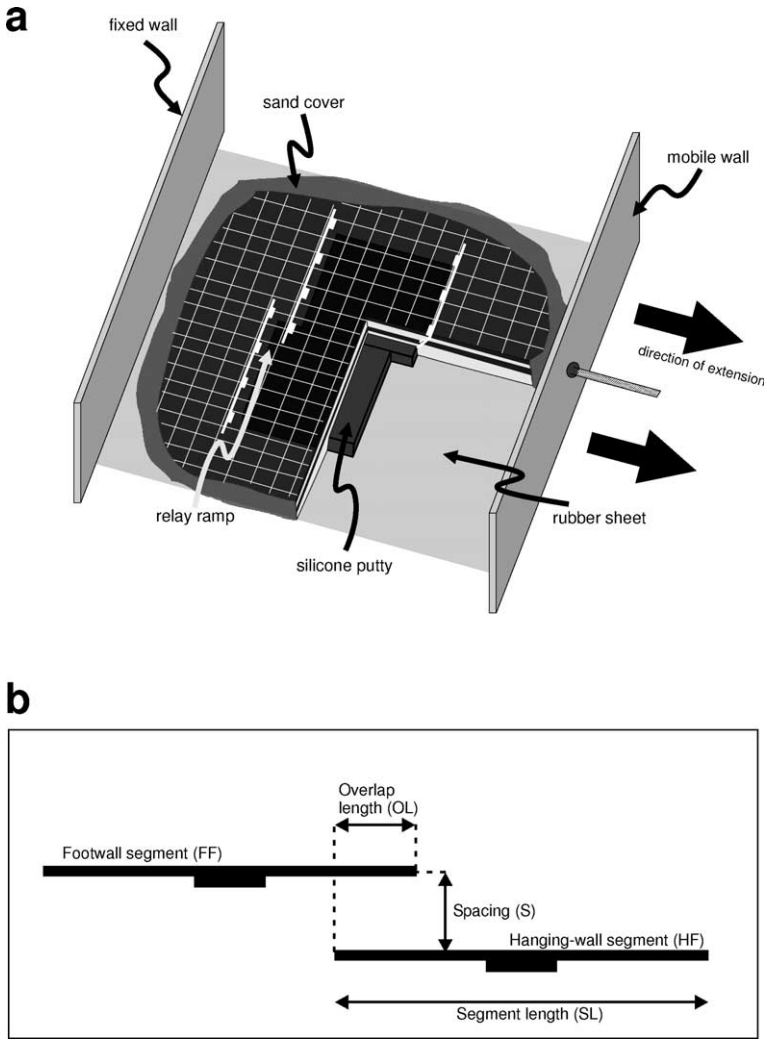

Fig. 2. (a) Sketch of the experimental apparatus and (b) parameters that define the geometry of the two fault segments in a relay ramp.

The main parameters that we varied during the experiments were (Fig. 2b): (a) the spacing between fault segments (*S*), (b) segment length (*SL*), (c) segment overlap length (*OL*) and (d) segment strike, relative to each other and also with regard to the direction of extension. Moreover, we tested: (e) left overstepping and right overstepping relay ramps and (f) asymmetric displacement profiles along the normal faults. In this case, the asymmetric displacement was achieved by varying the thickness of the silicone bars along the length of the bars. Because the deformation was focused at the sand–silicone interface, a thicker silicone bar corresponds to a higher displacement.

Extension in the models has been limited to 10 cm (corresponding to 20% stretching), to prevent tearing of the underlying rubber sheet. At the end of the experiments the models were impregnated with water and sliced parallel to the direction of extension to create fault perpendicular cross-sections of the overlap zones.

3. Results

3.1. General evolution of the experiments

The results of the experiments are listed in Table 1, which shows the characteristics of the observed overlap zones after the final amount of extension (10 cm) was reached. The final fault overlap length (*OL*) and the fault system length (FSL) were measured at the surface of the model, whereas the fault displacement (*D*) was measured along the cross-sections. FSL corresponds to the total length of the fault system, i.e. the summed length of the two segments minus the overlap length.

The general evolution of the relay ramps was characterized by three different stages (Fig. 3), here described.

(1) *Immature stage*. This stage consists of the onset and lateral propagation of faulting, marked by the development of isolated fault traces at the surface (Fig. 3a). The onset of faulting at the surface was usually observed after approximately 2 cm of extension. Apart from a flexural bend at the

Table 1
Summary of the different results and starting parameters of the experiments. The original overlap (*OO*) and the spacing (*S*) were implied by the silicone bars, the other parameters resulted from the extension

Exp. no.		FO	S	ST	FSL	AR	D	OO	Remarks
ZAV03	M	4.0	2.0	4.0	46			0	Interaction between M and A
	A	3.0	2.5	4.0	44			0	Ramps
ZAV04	M	6.5	2.5	5.5	34	3.7	2.0	0	FF deflects away from HF
	A	6.5	2.5	5.5	38	4.4	1.5	0	HF propagates towards FF
ZAV05	M	6.0	2.5	4.0	36	5.2	1.0	0	No breaching
	A	4.5	2.5	4.0	34	4.8	0.7	0	FF propagates towards HF
ZAV06	M	–	1.5	6.0	30	2.5	1.3	0	No ramp, continuous fault
	A	8.5	1.5	6.0	34	3.5	1.0	0	Breaching through splaying
ZAV07	M	–	1.5	5.8	34	2.9	1.0	0	No ramp, continuous fault
	A	–	2.0	5.8	36	3.1	1.7	0	No ramp, continuous fault
ZAV08	M	16.0	5.0	5.5	35	4.6	1.3	0	Interaction but no breaching
	A	–	2.0	5.5	40	3.6	1.0	0	No ramp, continuous fault
ZAV09	M	5.0	7.0	4.2	20	2.9	0.3	0	No interaction
	A	9.0	2.0	4.2	22	3.7	0.6	0	HF connects with FF
ZAV10	M	10.0	2.5	4.0	26	4.5	0.5	2	Relay ramp but no breaching
	A	7.0	2.5	4.0	26	4.1	0.7	0	FF propagates to HF
ZAV11	M	10.0	1.5	5.0	22	3.2	?	4	No signs of breaching
	A	11.0	2.5	5.0	22	3.3	?	4	No signs of breaching
ZAV12	M	–	1.5	5.0	20	2.0	1.2	4	HF too big; links with FF before latter developed
	A	12.0	4.5	5.0	23	3.5	1.0	4	No interaction
ZAV13	M	7.0	3.0	5.0	20	2.7	0.5	4	Curved faults due to interaction
	A	9.0	3.0	5.0	20	2.9	0.5	4	Curved faults due to interaction
ZAV14	M	7.0	4.0	4.8	22	3.0	0.33	0	Interaction??
	A	6.5	2.5	4.8	23	3.1	0.66	0	HF links with FF
ZAV15	M	10.5	3.5	3.7	25	4.8	0.8	0	
	A	5.0	2.5	3.7	23	3.8	0.8	0	
ZAV16	M	7.0	2.5	4.3	25	3.7	1.0	0	
	A	6.5	2.5	4.3	24	3.5	1.0	0	
ZAV17	M	12.0	5.0	4.3	24	4.2	1.0	0	
	A	5.0	1.5	4.3	24	3.4	0.8	0	Breaching through splaying
ZAV18	M	4.0	1.5	4.5	24	3.1	0.7	0	Small ramp breached by FF linking with HF

FO=final overlap; *S*=spacing; *ST*=thickness of sand cover; FSL=fault system length; *AR*=aspect ratio of faults; *D*=displacement; *OO*=original overlap of silicone bars; HF=hanging-wall fault; FF=footwall fault; all dimensional units are in cm.

model's surface, no precursors to faulting (like the development of extensional fractures) were observed. The top view pictures of the experiments at early stages (2 cm of extension) show that the faults usually started to form in the centre of the silicone bar and subsequently propagated towards the ends of the bar. However, small-displacement faults with the same lengths as the silicone bars also formed at early stages of the experiments. This suggests that the faults in the immature stage were either characterized by small displacements with respect to their fault lengths according to scaling laws for displacement and length (e.g. Schlische et al., 1996), or that the faults were characterized by a considerable vertical propagation before they reached the model's surface (e.g. Walsh et al., 2002). Further extension of the model increased the displacement along these fault segments, causing them to propagate laterally. When this propagation started, the fault length was no longer restricted to the length of the silicone bars, and free propagation outside the bar area started. None of the final fault lengths equalled the length of the underlying silicone bar, which implies that this free lateral propagation was observed in all the models.

(2) *Interaction stage*. The second stage was reached when the propagation of the segments was large enough to start the interaction process between nearby faults (Fig. 3b). This interaction marks the initiation of a relay ramp. Two fault segments were considered to be interacting when: (a) a tilt of the topography could be observed at the surface of the model between segments (this tilt corresponded to a bend or tilt of the layers in cross-section); (b) a deflection of the strike of one or both of the faults towards the relay was observed. The use of these criteria to infer fault interaction allows the comparison of the experimental results with data from natural examples at various scales (see below) (e.g. Acocella et al., 2000). Tilting of the layers inside the ramp was usually towards the footwall fault, with the angle of tilt being $\sim 5^{\circ}$.

(3) *Linkage stage*. The final stage in the evolution of relay ramps was reached when the two faults became hard linked and the relay ramp was broken or breached (Fig. 3c).

This stage was characterized by either the propagation of one of the main faults towards the other or by the development of a new connecting fault that splayed from one of the main faults and subsequently cut through the relay ramp. After 10 cm of extension, half of the experiments were either in the linkage stage or characterized by an incipient breaching (e.g. the propagation of one of the main faults towards the other).

3.2. Relationship between fault length, displacement and spacing

Incipient normal faults were often characterized by small displacements with respect to their fault length in the immature stage. To determine whether or not this remained the case during further evolution of the models, the relationship between fault length and displacement was evaluated and compared with known scaling laws (Fig. 4). This allowed us to test whether the fault triggering mechanism (i.e. using the basal silicone bars) impacted on the final fault shapes. Although in natural examples of relay ramps, the maximum displacement on the fault segments is rather located near the overlap zones than in the centre of the segments (Peacock and Sanderson, 1991, 1994), the fault displacements were measured in the centre of the silicone bars, as this is the place where the faults are usually observed to have nucleated. For 27 faults, the obtained relationship between segment length (L) and displacement (D) after 10 cm of extension is:

$$D = 0.0226L^{1.11} \quad (1)$$

For interacting fault segments, the fault system length (FSL) has been used for L, whereas for non-interacting faults L equalled the length of the individual faults. Faults that had reached the lateral boundaries of the sandbox have not been included in the calculation of this relation, because in such cases the fault growth would have been censored.

Fig. 5 shows the relationships between the spacing (S) of the modelled faults and their total length (fault system length, FSL, in Table 1). The experiments show two distinct domains, where the interaction (stage 2 described above) occurs and where it does not, as a function of these values. Given a certain total length of the faults, the interaction occurs if $S \ll$ FSL; for a given FSL, a larger spacing of fault segments results in no interaction. The 'interaction' and 'no-interaction' domains in Fig. 5 are separated by a transition zone, where the interaction is incipient. The best-fit line that separates the two domains is given by the equation:

$$S = 0.135\text{FSL} + 0.68 \quad (2)$$

Fig. 5 also displays two lines marking the transition between the interacting (below) and non-interacting (above) domains of experimental strike-slip faults (An, 1997) and extensional fractures and normal faults in Iceland (Acocella et al., 2000). The line from An (1997) shows that the minimum length of a strike-slip fault system is about 10 times the value of the spacing for interaction to occur, whereas the line from Acocella et al. (2000) suggests that this length is 14 times the spacing of the normal faults. Our data shows that the critical total fault length to have interaction or not is about eight times the spacing, slightly lower than the previous results.

3.3. The role of fault overlap length and spacing

During the propagation of the faults in the experiments it was observed that an initial overlap of the segments was reached around 3–4 cm of extension in the model runs. Fig. 6 shows the variation of the overlap distance of the normal faults as a function of the amount of extension. The initial underlapped segment geometries occurred only for relatively small strains (mostly <4 cm of extension), and could not be accurately plotted in Fig. 6.

The overlap length is mostly proportional to the amount of extension; nevertheless, at intermediate to late stages of extension, the slope of the curves sharply decreases. This indicates that, when a certain overlap length was attained (mostly between 40 and 70 mm of extension, roughly corresponding to the second evolutionary stage), the rate of propagation of the fault tips bordering the relay ramp decreased.

The role of fault spacing (S) on the final overlap length (FO) is shown in Fig. 7. Here both values are normalized to the fault length. The figure shows a generally proportional relation between FO and S, indicating that overlap zones characterized by larger fault spacing typically reach a greater overlap length.

This proportional relationship is no longer valid in cases where the fault spacing (S) is large compared with the fault length (SL) so that interaction no longer occurs ($S > 0.3SL$). In this case, the propagation of the overlapping fault segments will not be impeded by the mutual interaction between the faults, and therefore large overlap lengths are expected. This large overlap length is observed in experiments 12A and 17M, but not in experiment 9M (Fig. 7).

A small spacing with regard to the FSL ($S < 0.075$FSL) leads, in some cases, to the formation of a continuous fault, without the development of an overlap zone, as shown by the points plotted on the x-axis of Fig. 7. We believe that the thickness of the sand pack relative to the fault spacing may influence whether faults are continuous or not. This relation exists because faults propagate from the base of the model and a thicker sand pack allows greater opportunities for faults segmented at depth to link before reaching the surface. However, the sand thickness cannot be the only factor influencing the degree of fault linkage, as in experiment ZAV06, for the same sand thickness and spacing both continuous fault (06M) and segmented fault (06A) geometries developed.

Linear elastic fracture mechanical models show that the

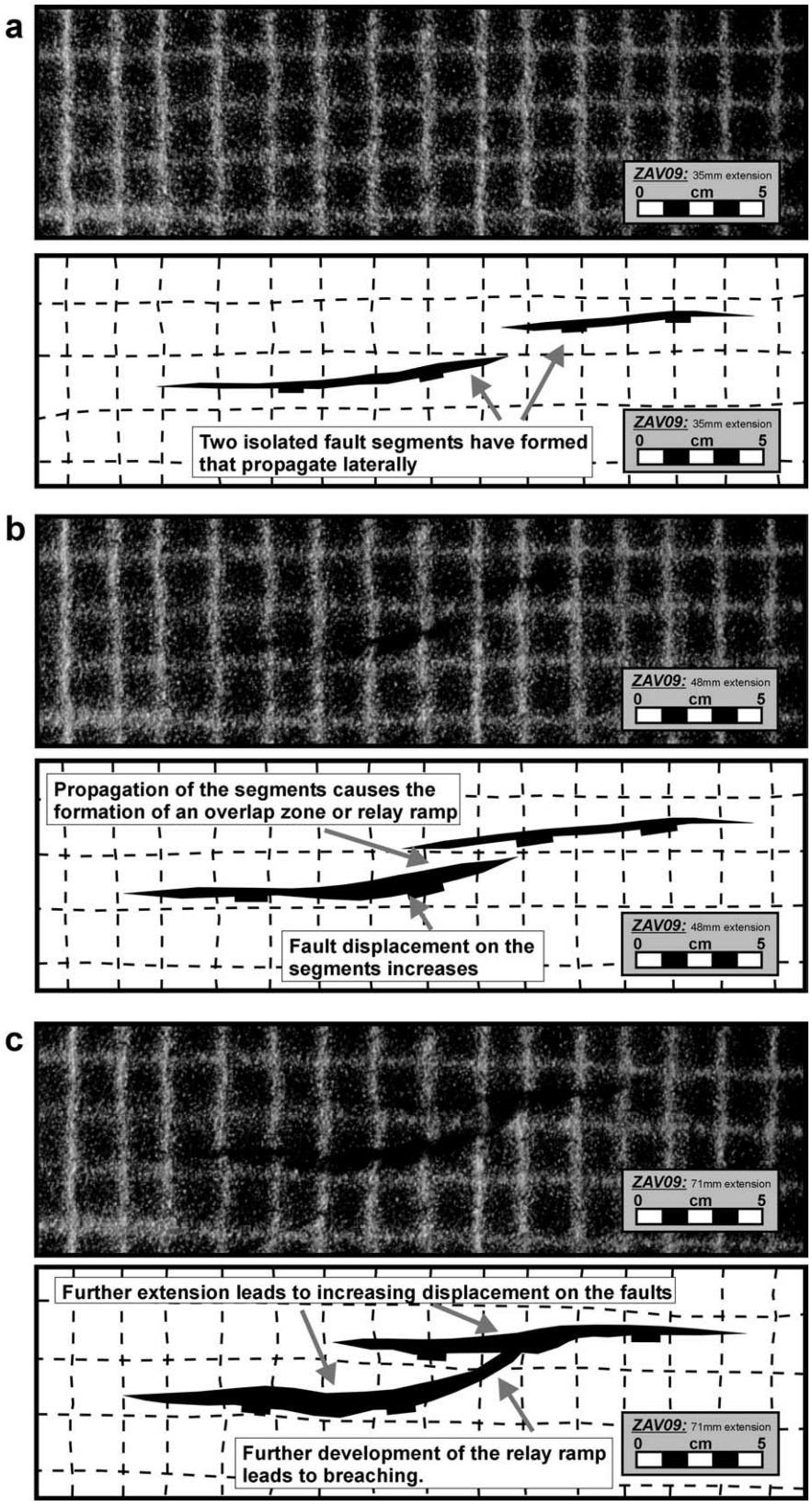

Fig. 3. Photographs and sketch maps of experiment ZAV09, showing the three different evolutionary stages observed in the modelling: the immature stage (a), the interaction stage (b) and the linkage stage (c). Linkage in this experiment was achieved through the propagation of the hanging-wall fault towards the footwall fault.

aspect ratio (A) of the fault (i.e. length/height) controls the overlap length to spacing ratio of a relay ramp (Willemse, 1997). Theoretical curves of faults with A of 2 and 4 (from Willemse, 1997) have, therefore, been added to Fig. 7. Aspect ratios for experimental faults varied between 2.5 and 5.2, plotting around the theoretical curve of Willemse (1997) for faults with $A=4$. Despite this general trend, the data are scattered around the theoretical curves. Some points with $A\sim3$ (11M, 11A, 17A) plot to the left of the theoretical curve with $A=4$.

Fig. 8 shows the distribution of the overlap length to spacing ratio of the experimental overlap zones during the second evolutionary stage (not including continuous faults and the non-interacting faults). The mean ratio is 3.12 and 95% of the examples lie between 1.75 and 6.

3.4. Relay ramp breaching

In our experiments, 11 examples (or 50%) of the relay ramps had breached, or were in the process of being breached, when the final amount of extension was attained (i.e. 10 cm, corresponding to a stretching factor of 20%) (e.g. Figs. 9 and 10). In particular: (1) 55% of the breaching occurred through the propagation of the hanging-wall fault towards the footwall fault; (2) 27% occurred through the propagation of the footwall fault towards the hanging-wall fault; (3) in 18% of the cases, the breaching was accomplished by a new fault that cut across the ramp. Hanging-wall fault to footwall fault propagation was thus the most common form of linkage, even though both the hanging-wall and the footwall faults started to form at the same time. The further development of especially the hanging-wall fault in most of the cases resulted in the development of a depression at the centre of the hanging-wall fault trace. After the hanging-wall fault had propagated to the footwall fault, a second depression developed near the point of intersection. This central depression usually became the largest of the whole system (Fig. 10a).

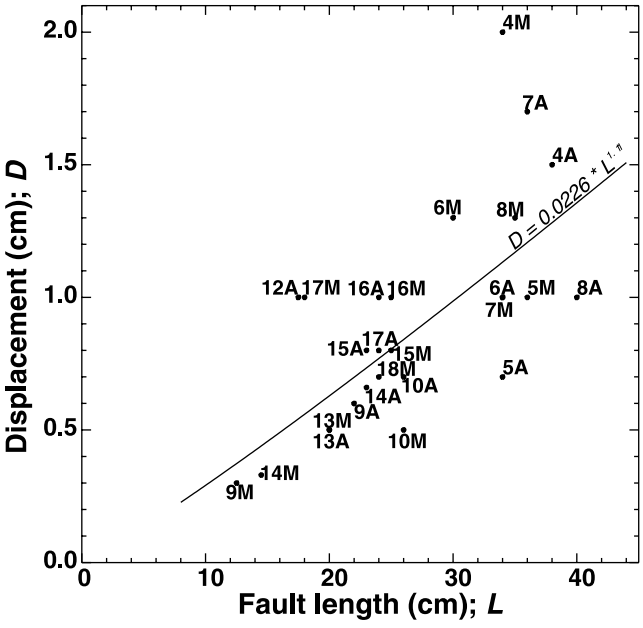

Fig. 4. Relationship between the fault lengths of the modelled faults and the displacement along that fault. Displacement was measured on a cross-section through the centre of one of the segments. Numbers refer to the experiment's name in Table 1.

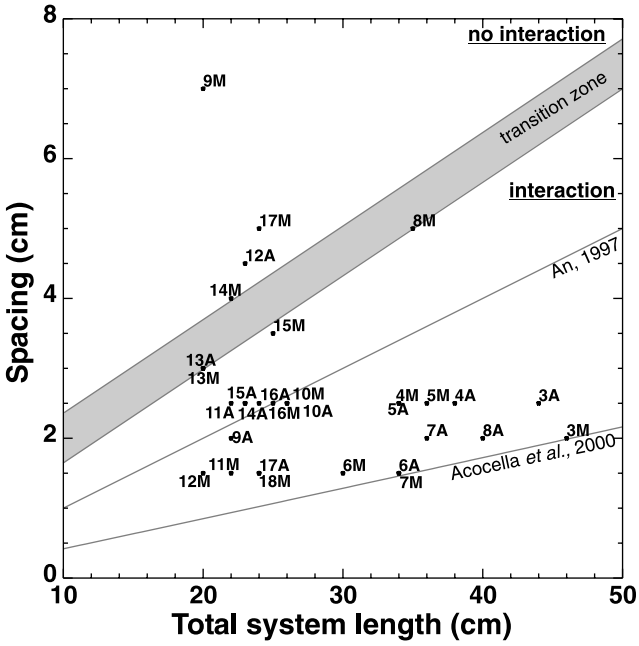

Fig. 5. Relationship between the spacing of two fault segments and the length of the total system (FSL). The upper left corner of the graph corresponds to an area where no interaction occurs and the lower right corner is marked by interaction. The grey zone is a transition zone between both areas. The line curves correspond to transitions observed in other studies.

When the footwall fault propagated towards the hanging-wall fault, both faults showed a similar displacement. This resulted in the development of two similarly sized depressions, at the centre of the footwall fault and at the centre of the hanging-wall fault. After the footwall fault connected with the hanging-wall fault, the depressions remained separate, without connecting in the former ramp area, where an intra basin high structure (Schlische, 1995) was observed (Fig. 10b).

The breaching of the relay ramp by means of a connecting fault was usually observed when the faults were closely (i.e. <2 cm or <0.0625 normalized to FSL) spaced (e.g. ZAV06A and ZAV17A). In the case of experiment ZAV17A, the displacement gradient along the hanging-wall fault increased abruptly just outside the overlap zone, and decreased again within it. At exactly this location a new breaching fault splayed off the hanging-wall fault and propagated across the relay ramp to link up with the footwall fault.

In some cases (e.g. experiments ZAV06M, ZAV07 and ZAV08A), the experimental faults linked at very early stage and low strains, before reaching the surface of the sand

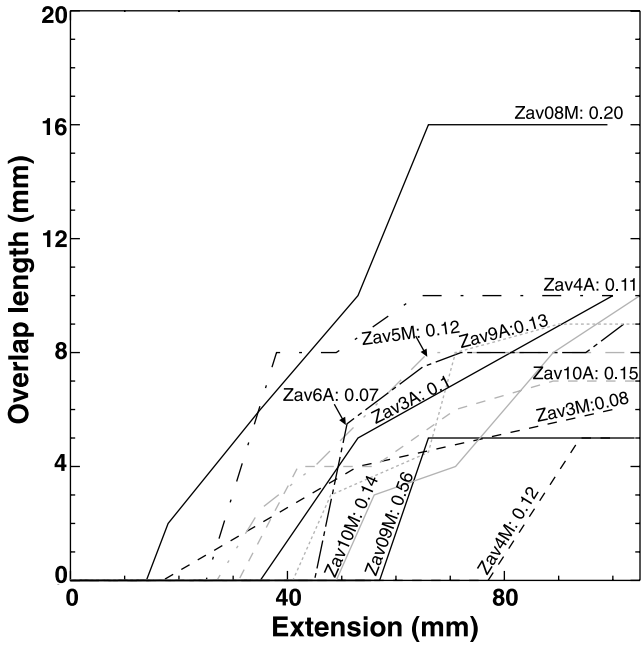

Fig. 6. Overlap length of the two fault segments of the relay ramp in relation to the amount of extension. The numbers after the experiment names correspond to the ratio of fault spacing and segment length. Graphs have been linearly interpolated between different measurements.

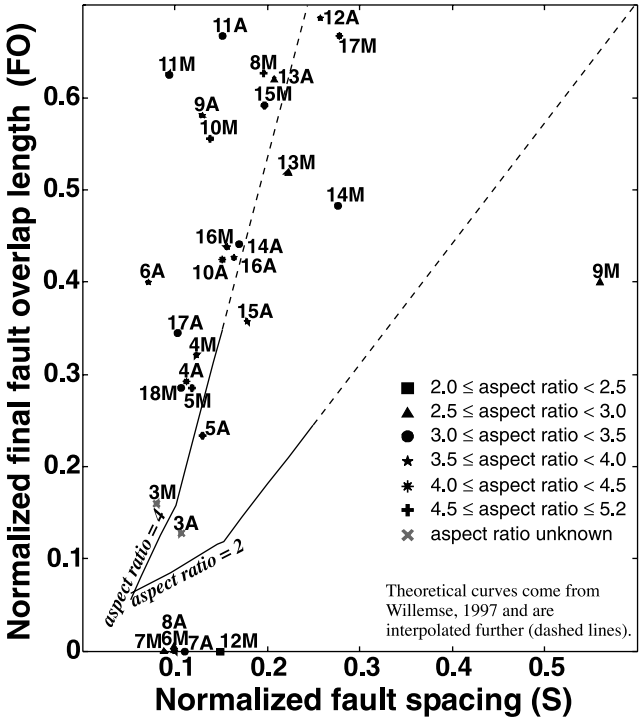

Fig. 7. Relationship between fault overlap length and spacing of the experimental overlap zones. Both values are normalized to the segment length. The line curves come from Willemse (1997) and correspond to the modelled relationship for faults with a certain aspect ratio that are characterized by a uniform stress drop along the fault trace.

cover. As a result, a continuous, sinuous fault formed (Fig. 11). Nevertheless, these faults were associated with two separate depressions, corresponding to activity of the former interacting faults. One depression was located in the centre of the former hanging-wall fault and the other was located at the former footwall fault. The latter depression, being the largest, was slightly shifted towards the bend (Fig. 11). After relay ramp breaching fault tips continued to propagate, albeit at a lower rate than prior to breaching, and the vestigial splays continued to accommodate extension (Figs. 9 and 11).

When we imposed a strike of the main faults that was oblique to the extension directions, the faults followed this oblique direction inside the silicone putty bars, but adopted a geometry outside the bars that was again approximately perpendicular to the direction of extension. In the experiments this resulted in left-oblique left-stepping faults and right-oblique right-stepping faults to form a more closed geometry of the ramps (faults growing towards each other), whereas for right-oblique left-stepping faults and left-oblique right-stepping faults, the relay zones were more ‘open’ i.e. faults slightly diverging (Fig. 12). Changing the overstep direction did not have any influence on the overlap length to spacing ratios of the experimental overlap zones.

4. Discussion of the experiments

Three stages of relay ramp evolution have been identified in the experiments: immature, interacting and linkage. These correspond, respectively, to stages 1, 2 and 3–4 in the evolution scheme proposed by Peacock and Sanderson (1991), based on the study of natural relay ramps. The models did not show a significant development of secondary fractures in the relay ramps, which marks the onset of the breaking down of the relay ramp and forms the third evolutionary stage of Peacock and Sanderson (1991). In two of the experiments, the development of a connecting fault is typical of their third stage, but in these cases only the propagation of a well-defined single fault was observed, and not the breakdown of the relay ramp by a process of secondary faulting.

The small amount of extension (3–4 cm, corresponding to a stretching factor of 6–8%) typically required to initiate fault interaction in the experiments suggests that the immature stage was transient and short lived. During the interacting stage, the overlap lengths of the faults forming the relay ramps increased and then remained constant with no fault propagation. This lack of propagation is consistent with mechanical models of interacting normal and strike-slip faults, which suggest that interacting underlapping faults enhance each other’s propagation, whereas overlapping faults inhibit their reciprocal propagation (Pollard et al., 1982; Pollard and Aydin, 1984; Aydin and Schultz, 1990; Willemse et al., 1996; Crider and Pollard, 1998). This results in an initial increase of the propagation energy (during the underlapping configuration), followed by a

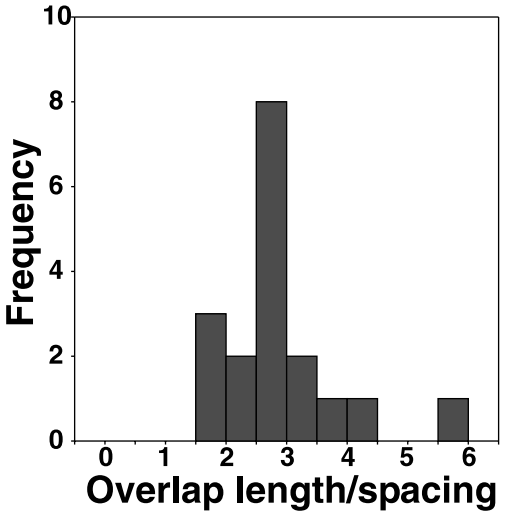

Fig. 8. Frequency distribution of the overlap/spacing ratio of the different experimental relay ramps ($n=22$). Values cluster around 3, with a mean value of 3.12.

decrease of this energy (during the overlapping configuration).

The experimental displacement–length relationship for the fault segments forming the overlap zones is $D=0.0226L^{1.11}$ (Fig. 4). In natural fault systems, the value of the exponent n varies between 1 and 2 (Walsh and Watterson, 1988; Cowie and Scholz, 1992; Gillespie et al., 1992; Gudmundsson, 1992; Dawers et al., 1993), whilst in analogue models with plaster, $n=0.93$ (Mansfield and Cartwright, 2001). The displacement–length relation obtained from our experiments is not fully accurate for two reasons: (1) there is a large data scatter in the graph, and (2) our data span only one order of magnitude. Nevertheless, taking into account that these values also depend on material properties (Cowie and Scholz, 1992), our $n=1.11$ appears to be consistent with values obtained from natural systems. This suggests that the above described small fault displacements relative to the fault lengths in our models are indeed readjusted to a normal displacement at later stages. The large scatter ($R^2=0.5$) of the data in Fig. 4 may be explained as being caused by the dependence of the relation on several factors (spatial stress variations along a fault, frictional strength along a fault, inelastic deformation at fault tips, e.g. Bürgmann et al., 1994; Mansfield and Cartwright, 2001) that interplay with each other, not least the measurement errors in determining D and L. The latter have been evaluated being, respectively, 10–15% and 1.5–2.5%. Also the effects of fault interaction and linkage can cause the observed scatter (Peacock and Sanderson, 1991).

The interaction between overlapping faults occurred only for a certain threshold of the initial FSL/S ratio (Fig. 5), similar to what has previously been observed in experimental strike-slip faults (An, 1997) and natural extensional fractures and normal faults (Acocella et al., 2000). The experimental threshold (FSL/$S=8$) is almost half of the one obtained in nature (FSL/$S=14$) for normal faults. The dependence of this relation on rheology and scale could explain the difference between our experimental threshold and that in nature. The difference between both could even be larger depending on our experimental resolution (estimated to be $\sim 1^\circ$ for the tilt). It is difficult to estimate how a higher resolution of the experiments would influence the location of the transition zone in Fig. 5.

The relationship between the overlap length and the spacing of the modelled normal faults (Fig. 7) can be explained by the variations in the propagation force of the two segments. The decrease in the propagation force is larger for closely spaced fractures than for widely spaced

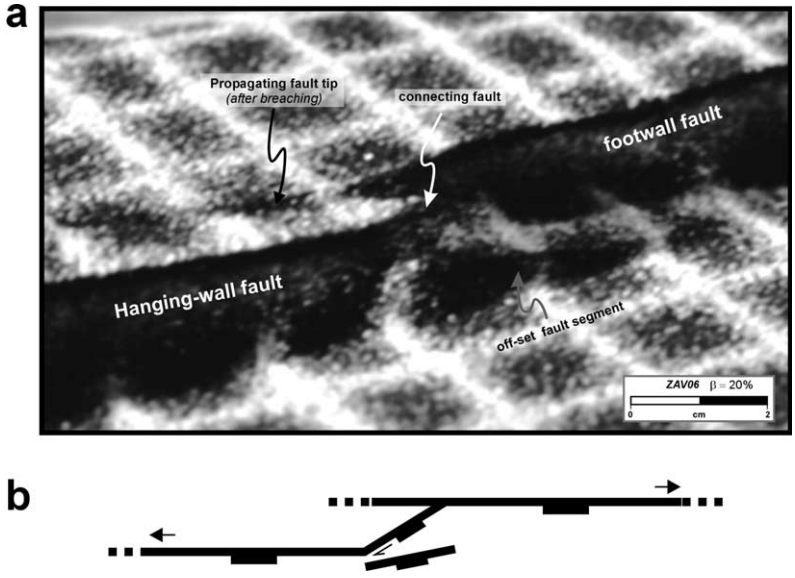

Fig. 9. (a) Oblique photograph of experiment ZAV06A. This model is an example of a relay ramp that is breached by a connecting fault. The picture illustrates the propagation of the fault tips after the relay ramp was breached. (b) Line drawing of the observed fault geometry.

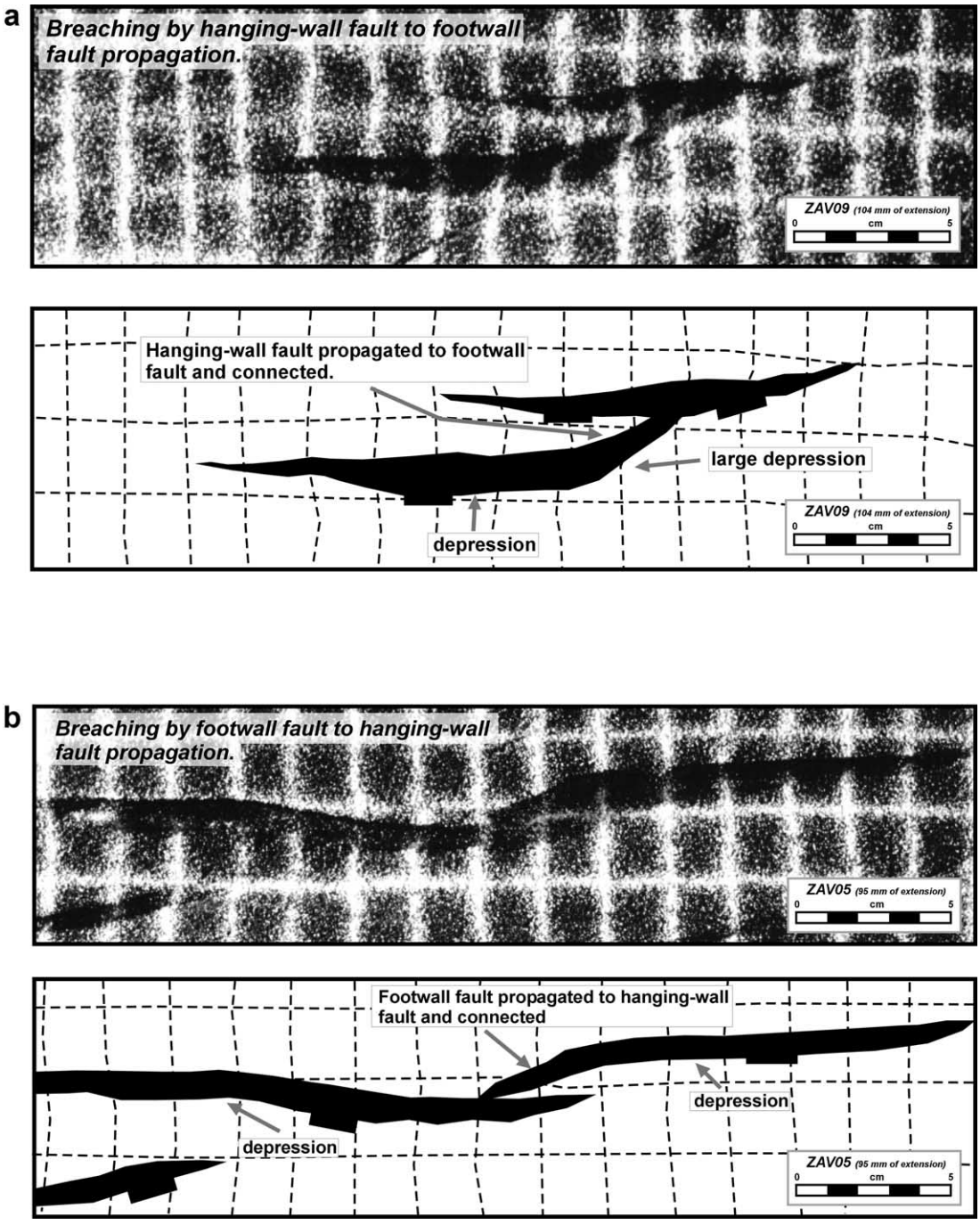

Fig. 10. (a) Example of a relay ramp breached by the propagation of the hanging-wall fault towards the footwall fault. (b) Example where breaching occurred through the propagation of the footwall fault to the hanging-wall fault. Arrows indicate the different depressions that have formed.

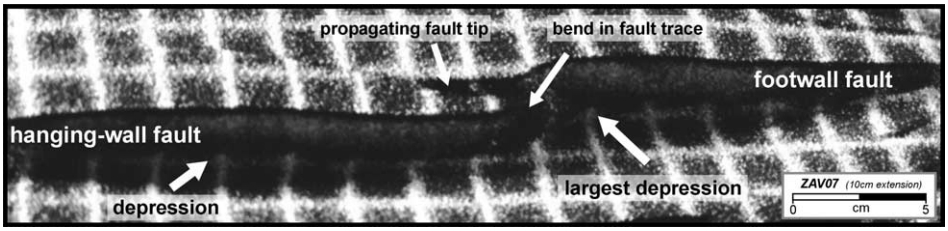

Fig. 11. Oblique photograph of experiment ZAV07A. The experiment was characterized by a connection of the two stepping fault segments before the faults reached the surface of the sand cover. Note the occurrence of the two depressions and the propagation of the fault tip of the footwall segment.

fractures (Pollard and Aydin, 1984). This implies that closely spaced faults are more subject to the propagation impediment resulting from fault interaction, which finally inhibits the further propagation of the faults in the relay ramp. Faults that are more widely spaced will experience the same propagation impediment only when larger overlap lengths have been attained (Pollard and Aydin, 1984).

A small spacing of the silicone bars can either result in the formation of a relay ramp or a continuous fault with a bend, even under the same experimental boundary conditions (e.g. experiments 6A and 6M). This shows the difficulty of defining a unique solution for the fault linkage process in the case of small S compared with FSL. The development of a relay ramp or a continuous fault at early stages might be influenced by small perturbations in the model. For example, Mansfield and Cartwright (2001) argue that small mechanical heterogeneities in their models might have a significant impact on the finite geometry of fault displacements of their experiments.

Willemse (1997) suggests that the aspect ratio (length/height) of the faults influences their mechanical interaction, as the stress field perturbation around a fault is larger for tall faults (i.e. with a low aspect ratio) than for short faults (i.e. with a high aspect ratio). The height of our experimental faults was determined by the thickness of the sand pack. Once faults had reached the model's surface, their height remained constant, while their length still increased. This implies that the aspect ratios of the experimental faults increased with increasing extension. As a result, calculating the aspect ratio from the final fault length and fault height, an overestimation of the aspect ratio is calculated. It is, therefore, not possible to compare the experimental observations with the available data on the aspect ratio of interacting faults.

The length/width ratios of the experimental relay ramps cluster around a mean value of 3.12 (Fig. 8a), suggesting that relay ramps have certain preferred geometries. The distribution in Fig. 8a is in agreement with the one obtained from bridges between extensional fractures and relay ramps between normal faults on the oceanic ridge of Iceland (Acocella et al., 2000). For 88% of the Icelandic relay ramps, the ratio was between 2 and 6, with a mean value of 3.5. Also, a similar mean value (3.5) was obtained in field studies and in sand-box experiments on pull-aparts between strike-slip fault segments (Aydin and Nur, 1982; Basil and Brun, 1999). These data show a consistency in the aspect ratio of interaction zones between normal faults (forming relay ramps) and strike-slip faults (forming pull-apart basins), at scales differing several orders of magnitude (from 10^{-2} to 10^{5} m). This suggests that steps in extensional and strike-slip domains have comparable geometries, regardless of the scale and fault style.

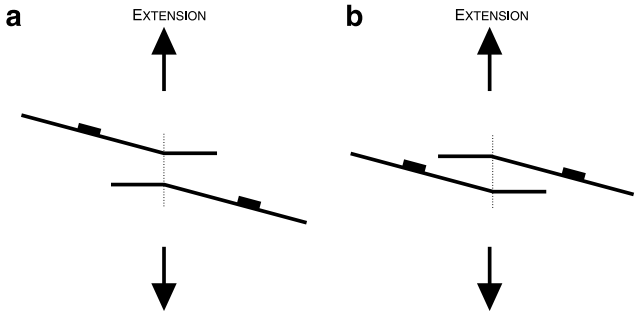

Fig. 12. Schematic illustration of the difference in overlap zone geometry between (a) left-oblique right-stepping faults, where an 'open' overlap zone developed, and (b) left-oblique left-stepping faults, where the geometry was more 'closed'.

In the experiments, 55% of the breached relay ramps were characterized by hanging-wall fault to footwall fault propagation, 27% by footwall fault to hanging-wall fault propagation, and only 18% by the development of a new connecting fault. However, the most frequent way of breaching in nature (Table 2) appears to be through the propagation of the footwall fault towards the hanging-wall fault. The development of a new fault connecting the two relaying fault segments has been rarely reported for natural cases (e.g. Ferrill et al., 1999; Peacock and Parfitt, 2002). Ferrill et al. (1999) related the mode of relay ramp breaching to the displacement gradients on the main faults. Steep displacement gradients resulting from large displacements at the fault tips without proportional propagation of this tip would favour breaching by a connecting fault, whereas in the other cases one of the main faults is more likely to propagate. Nevertheless, a similar relationship between large displacement gradients at the fault tip and the development of a connecting fault was not observed in the experiments.

The overall geometry, structure and evolution of the experimental overlap zones show close similarities with natural examples and existing conceptual models of relay ramp evolution. Nevertheless, an aspect of the evolution of the relay ramps observed in the experiments has not been described in nature. This concerns the propagation of the main fault tips even after the relay ramp is breached. Existing models of relay ramp evolution (Peacock and Sanderson, 1991, 1994) imply that as soon as a hard connection is formed between the main offset faults, this connection will take over all displacement in the ramp, causing the ramp and the unused fault tips to become abandoned as strain is focused on the newly formed fault. Several experiments were characterized by post-linkage propagation of the fault tips at the relay ramp (e.g. ZAV06A in Fig. 9). Even experiments where a continuous fault was formed before it reached the surface of the model (e.g. ZAV07A in Fig. 11) showed the propagation of one or both of the main faults at the bend. In nature, the final geometry of both (the pre-linkage fault tip propagation and the post-linkage fault tip propagation) linkages may be identical (Fig. 13). Nevertheless, their evolution may be significantly different; in one case (Fig. 13a), the final stage is achieved through the propagation of the tips of the faults, until one reaches the other and the remaining tip is abandoned

Table 2
Overlap and spacing data of several natural normal fault systems

Area	Location	Geometry (m)		BT[a]	Reference
		Overlap	Spacing		
Canyonlands, Utah	SOB Hill relay zone	360	120	N	Trudgill and Cartwright (1994)
		360	140	N	Trudgill and Cartwright (1994)
	Twin Valleys region	100	66.67		Trudgill and Cartwright (1994)
Greenland	Hold With Hope	250000	100000		Peacock et al. (2000b)
North Sea Rift	Moray Firth	58536	29268		Morley et al. (1990)
	Argyll and Auk Fields	24390	12195		Morley et al. (1990)
	Argyll field	9600	4000		Morley et al. (1990)
Northeast Idaho	Beaverhead fault	16666	4583	F	Anders and Schlische (1994)
Newark Basin		14444	7777	N	Anders and Schlische (1994)
Hawaii	Kilauea Volcano	1034	689	N	Peacock and Parfitt (2002)
		1379	603	C	Peacock and Parfitt (2002)
Atalanti		1666	1666	N	Gawthorpe and Hurst (1993)
Northern North Sea	Strathspey–Brent–Statfjord	2941	1470	F	McLeod et al. (2000)
		1666	1111	F	McLeod et al. (2000)
		3333	2222	F	McLeod et al. (2000)
		122	44.44	F	Walsh et al. (1999)
		1200	250	B	Walsh et al. (1999)
		1333	111	N	Walsh et al. (1999)
Kenia	Lokichar Fault	4210	3684	F	Morley (2002)
Kilve, Somerset		0.90	0.15	C	Peacock and Sanderson (1994)
		0.75	0.08	N	Peacock and Sanderson (1994)
		0.27	0.03	F	Peacock and Sanderson (1994)
		0.90	0.26	F	Peacock and Sanderson (1994)
Watchet		0.64	0.14	B	Peacock and Sanderson (1994)
Central Graben	Olaf Fault	5454	3333	N	Cartwright (1991)
Central Graben	Gorm Fault Zone	1818	2424	N	Cartwright (1991)
	Coffee Soil Fault	2424	1212	F	Cartwright (1991)
Feda Graben		1818	1515	N	Cartwright (1991)
North Gulf of Evvia		2083	1250	N	Roberts and Jackson (1991)
Gulf of Corinth		2500	833	N	Roberts and Jackson (1991)
		1666	833	N	Roberts and Jackson (1991)
		5416	1666	N	Roberts and Jackson (1991)
		5416	1666	N	Roberts and Jackson (1991)
Cumbria, England		34.72	8.33	N	Barnett et al. (1987)
Aegean Region	Lastros fault zone	263	200	C?	Stewart and Hancock (1991)
Aegean Region	Yavansu fault zone	242	136	H	Stewart and Hancock (1991)
Abruzzo	Fiamignano fault	17727	9545	N	Cowie and Roberts (2001)
Abruzzo		27272	8181	N	Cowie and Roberts (2001)
Abruzzo		13636	7500	N	Cowie and Roberts (2001)
Karstryggen	Marcusdal Ramp	5294	4411	N	Larsen (1988)
South Yorkshire	Rockingham Colliery	52.63	105	N	Huggins et al. (1995)
Derbyshire	Glapwell Colliery	44.44	22.22	N	Huggins et al. (1995)
South Yorkshire	Denaby Main Colliery	14.71	11.76	N	Huggins et al. (1995)
South Yorkshire	Silverwood Colliery	130	16.00	N	Huggins et al. (1995)
Northumberland	Daisyhill coal site	166	72.22	N	Huggins et al. (1995)
North Derbyshire	Markham Colliery	194	41.18	N	Huggins et al. (1995)
Central North Sea		642	164	N	Childs et al. (1995)
Northern North Sea		1043	565	F	Childs et al. (1995)

[a] Breaching type: N=no breaching; C=connecting fault; H=hanging wall fault to footwall fault propagation; F=footwall fault to hanging-wall fault propagation; B=both faults propagated towards each other.

(Acocella et al., 2000, and references therein); in the other case (Fig. 13b) the same final configuration is achieved by an early propagation of one of the tips, while the other develops only after linkage has occurred. The same final configuration of linking normal faults may, therefore, be the result of different processes, related to a pre- and/or a post-linkage propagation of one or two of the fault tips.

In the experiments, the fact that the main faults continue to propagate even after a hard linkage structure has formed suggests that, shortly after breaching, the new hard connection is not yet able to transfer all the displacement between the stepping fault segments. Breaching as such does not imply the sudden cessation of activity in the relay ramp, and as such it is not an instantaneous process. In this

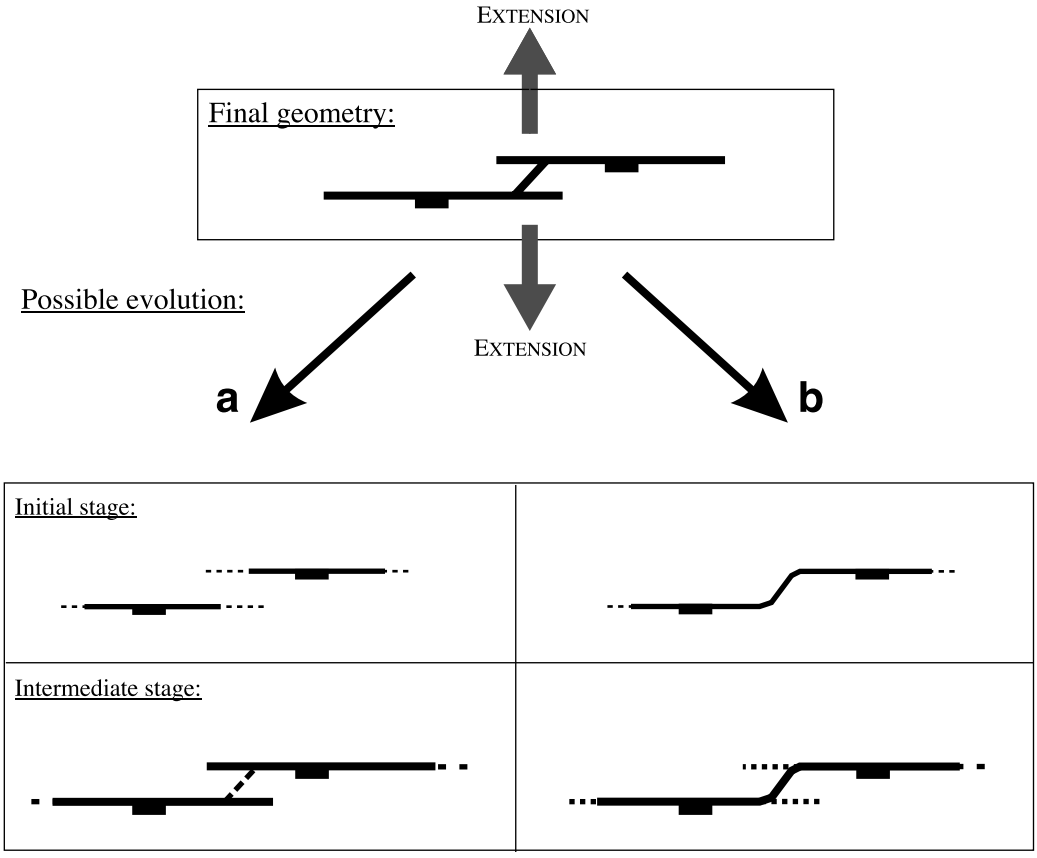

Fig. 13. Comparable final geometry can result from relay ramps breaching by (a) a connecting fault and (b) fault propagation at bends in a continuous fault. The dashed lines in the figure represent propagating faults.

framework, it could be useful to consider the possibility of a fifth evolution stage in the evolutionary scheme of Peacock and Sanderson (1991), being the post-breaching stage.

We have only been able to observe the fault evolution at the surface of our models, and this is a limitation. The vertical propagation of the faults from the base of the model (at the silicone bars, where the faults nucleated) to the top surface could explain the initially large fault lengths that have been observed in the models (e.g. Walsh et al., 2002). Also, in later evolution stages the observed fault growth at the model's surface could still be characterized by propagation out of the inspection plane; however, from the large aspect ratio's of the faults in our models, we believe that mainly in-plane propagation has been observed (e.g. Walsh et al., 2003).

5. Conclusions

Overlap zones with initially controlled fault geometries can be simulated using sandbox models containing basal silicone bars. The experimental relay ramps evolved in three stages, characterized by the growth of normal faults, their interaction and linkage. Interaction and linkage between fault segments has been observed only when the total combined length of the faults was larger than eight times their spacing. The length to width ratio of the overlap zones during the interaction stage showed preferred geometries, clustering around three. Three common ways of relay ramp breaching occurred in the experiments: i.e. hanging-wall fault to footwall fault propagation, footwall fault to hanging-wall fault propagation and the development of a new connecting fault. Hanging-wall fault to footwall fault propagation was the most common in the experiments, unlike in natural examples. The propagation of the fault tips was observed both before and after the linkage stage. The models evolved in a similar fashion to natural examples of relay ramps and are considered reliable analogues. Nevertheless, the further propagation of the fault tips after the linkage has not been described in nature and constitutes a new observation of evolution of extensional relay ramps.

Acknowledgements

R Hus is funded through an IWT-grant. The constructive reviews provided by Andy Nicol and David Peacock have been very helpful, and greatly improved the manuscript. Fig. 1 has been reprinted from Earth-Science Reviews, Vol. 58, no. 1–2, D.C.P. Peacock, Propagation, interaction and

linkage in normal fault systems, pp. 121–141, Copyright (2002), with permission from Elsevier.

References

Acocella, V., Faccenna, C., Funiciello, R., Rossetti, F., 1999. Sand-box modelling of basement-controlled transfer zones in extensional domains. Terra Nova 11, 149–156.

Acocella, V., Gudmundsson, A., Funiciello, R., 2000. Interaction and linkage of extension fractures and normal faults: examples from the rift zone of Iceland. Journal of Structural Geology 22, 1233–1246.

An, L., 1997. Maximum link distance between strike-slip faults: observations and constraints. Pure and Applied Geophysics 150, 19–36.

Anders, M.H., Schlische, R.W., 1994. Overlapping faults, intrabasin highs, and the growth of normal faults. The Journal of Geology 102, 165–180.

Aydin, A., Nur, A., 1982. Evolution of pull-apart basins and their scale independence. Tectonics 1, 91–105.

Aydin, A., Schultz, R., 1990. Effect of mechanical interaction on the development of strike-slip faults with echelon patterns. Journal of Structural Geology 12, 123–129.

Barnett, J.A.M., Mortimer, J., Rippon, J.H., Walsh, J.J., Watterson, J., 1987. Displacement geometry in the volume containing a single normal fault. Bulletin of the American Association of Petroleum Geologists 71, 925–937.

Basil, C., Brun, J.P., 1999. Transtensional faulting patterns ranging from pull-apart basins to transform continental margins: an experimental investigation. Journal of Structural Geology 21, 23–37.

Bürgmann, R., Pollard, D., Martel, S.J., 1994. Slip distributions on faults: effects of stress gradients, inelastic deformation, heterogeneous host-rock stiffness, and fault interaction. Journal of Structural Geology 16, 1675–1690.

Cartwright, J., 1991. The kinematic evolution of the Coffee Soil Fault, in: Roberts, A.M., Yielding, G., Freeman, B. (Eds.), The Geometry of Normal Faults Geological Society Special Publication, 56, pp. 29–40.

Childs, C., Easton, S.J., Vendeville, B.C., Jackson, M.P.A., Lin, S.T., Walsh, J.J., Watterson, J., 1993. Kinematic analysis of faults in a physical model of growth faulting above a viscous salt analogue. Tectonophysics 228, 313–329.

Childs, C., Watterson, J., Walsh, J.J., 1995. Fault overlap zones within developing normal fault systems. Journal of the Geological Society of London 152, 535–549.

Clifton, A.E., Schlische, R.W., Withjack, M.O., Ackermann, R.V., 2000. Influence of rift obliquity on fault-population systematics: results of experimental clay models. Journal of Structural Geology 22, 1491–1509.

Coskun, B., 1997. Oil and gas fields—transfer zone relationships, Thrace Basin, NW Turkey. Marine and Petroleum Geology 14, 401–416.

Cowie, P., Roberts, G.P., 2001. Constraining slip rates and spacings for active normal faults. Journal of Structural Geology 23, 1901–1915.

Cowie, P.A., Scholz, C.H., 1992. Physical explanation for the displacement–length relationships of faults using a post-yield fracture mechanics model. Journal of Structural Geology 14, 1133–1148.

Crider, J.G., Pollard, D.D., 1998. Fault linkage: three-dimensional mechanical interaction between echelon normal faults. Journal of Geophysical Research 103, 24373–24391.

Dawers, N.H., Anders, M.H., Scholz, C.H., 1993. Growth of normal faults: displacement–length scaling. Geology 21, 1107–1110.

Dooley, T., McClay, K., 1997. Analog modeling of pull-apart basins. Bulletin of the American Association of Petroleum Geologists 81, 1804–1826.

Faccenna, C., Nalpas, T., Brun, J.P., Davy, P., 1995. The influence of pre-existing thrust faults on normal fault geometry in nature and experiments. Journal of Structural Geology 17, 1139–1149.

Ferrill, D.A., Stamatakos, J.A., Sims, D., 1999. Normal fault corrugation: implications for growth and seismicity of active normal faults. Journal of Structural Geology 21, 1027–1038.

Gawthorpe, R.L., Hurst, J.M., 1993. Transfer zones in extensional basins: their structural style and influence on drainage development and stratigraphy. Journal of the Geological Society of London 50, 1137–1152.

Gillespie, P.A., Walsh, J.J., Waterson, J., 1992. Limitations of dimension and displacement data from single faults and the consequences for data analysis and interpretation. Journal of Structural Geology 14, 1157–1172.

Gudmundsson, A., 1992. Formation and growth of normal faults at the divergent plate boundary in Iceland. Terra Nova 4, 464–471.

Gupta, A., Scholz, C.H., 2000. A model of normal fault interaction based on observations and theory. Journal of Structural Geology 22, 865–879.

Horsfield, W.T., 1977. An experimental approach to basement-controlled faulting. Geologie en Mijnbouw 56, 363–370.

Huggins, P., Watterson, J.J., Walsh, J.J., Childs, C., 1995. Relay zone geometry and displacement transfer between normal faults recorded in coal-mine plans. Journal of Structural Geology 17, 1741–1755.

Larsen, P.H., 1988. Relay structures in a Lower Permian basement-involved extension system, East Greenland. Journal of Structural Geology 10, 3–8.

Le Calvez, J.H., Vendeville, B.C., 2002. Experimental designs to model along-strike fault interaction. Journal of the Virtual Explorer 6, 7–23.

Macdonald, G.A., 1957. Faults and monoclines on Kilauea Volcano, Hawaii. Bulletin of the Geological Society of America 68, 269–271.

Mandl, G., 1988. Mechanics of Tectonic Faulting: Models and Basic Concepts. Elsevier. 407pp.

Mansfield, C., Cartwright, J., 2001. Fault growth by linkage: observations and implications from analogue models. Journal of Structural Geology 23, 745–763.

Mauduit, T., Dauteuil, O., 1996. Small-scale models of oceanic transform zones. Journal of Geophysical Research 101, 20195–20209.

McClay, K.R., White, M.J., 1995. Analogue modelling of orthogonal and oblique rifting. Marine and Petroleum Geology 12, 137–151.

McClay, K.R., Dooley, T., Whithouse, P., Mills, M., 2002. 4-D evolution of rift systems: insight from scaled physical models. Bulletin of the American Association of Petroleum Geologists 86, 935–959.

McLeod, A.E., Dawers, N.H., Underhill, J.R., 2000. The propagation and linkage of normal faults: insights from the Strathspey–Brent–Statfjord fault array, northern North Sea. Basin Research 12, 263–284.

Morley, C.K., 2002. Evolution of large normal faults: evidence from seismic reflection data. Bulletin of the American Association of Petroleum Geologists 86, 961–978.

Morley, C.K., Nelson, R.A., Patton, T.L., Munn, S.G., 1990. Transfer zones in the East African Rift System and their relevance to hydrocarbon exploration in rifts. Bulletin of the American Association of Petroleum Geologists 74, 1234–1253.

Peacock, D.C.P., 1991. Displacements and segment linkage in strike-slip fault zones. Journal of Structural Geology 13, 1025–1035.

Peacock, D.C.P., 2002. Propagation, interaction and linkage in normal fault systems. Earth-Science Reviews 58, 121–142.

Peacock, D.C.P., Parfitt, E.A., 2002. Active relay ramps and normal fault propagation on Kilauea Volcano, Hawaii. Journal of Structural Geology 24, 729–742.

Peacock, D.C.P., Sanderson, D.J., 1991. Displacements, segment linkage and relay ramps in normal fault zones. Journal of Structural Geology 13, 721–733.

Peacock, D.C.P., Sanderson, D.J., 1994. Geometry and development of relay ramps in normal fault systems. Bulletin of the American Association of Petroleum Geologists 78, 147–165.

Peacock, D.C.P., Knipe, R.J., Sanderson, D.J., 2000a. Glossary of normal faults. Journal of Structural Geology 22, 291–305.

Peacock, D.C.P., Price, S.P., Whitham, A.G., Pickles, C.S., 2000b. The World's biggest relay ramp: Hold With Hope, NE Greenland. Journal of Structural Geology 22, 843–850.

Pollard, D.D., Aydin, A., 1984. Propagation and linkage of oceanic ridge segments. Journal of Geophysical Research 89, 10017–10028.

Pollard, D.D., Segall, P., Delaney, P.T., 1982. Formation and interpretation of dilatant echelon cracks. Bulletin of the Geological Society of America 93, 1291–1303.

Ramberg, H., 1981. Gravity, Deformation and the Earth's Crust, 2nd ed, Academic Press, London.

Roberts, S., Jackson, J., 1991. Active normal faulting in central Greece: an overview, in: Roberts, A.M., Yielding, G., Freeman, B. (Eds.), The Geometry of Normal Faults Geological Society Special Publication, 56, pp. 125–142.

Schlische, R.W., 1995. Geometry and origin of fault-related folds in extensional settings. Bulletin of the American Association of Petroleum Geologists 79, 1661–1678.

Schlische, R.W., Young, S.S., Ackermann, R.V., Gupta, A., 1996. Geometry and scaling relations of a population of very small rift-related normal faults. Geology 24, 683–686.

Schreurs, G., Hänni, R., Vock, P., 2001. Four-dimensional analysis of analog models: experiments on transfer zones in fold and thrust belts, in: Koyi, H.A., Mancktelow, N.S. (Eds.), Tectonic Modelling: A Volume in Honor of Hans Ramberg Geological Society of America, Memoir, 193, pp. 179–190.

Stewart, I.S., Hancock, P.L., 1991. Scales of structural heterogeneity within neotectonic normal fault zones in the Aegean region. Journal of Structural Geology 13, 191–204.

Trudgill, B.D., Cartwright, J.A., 1994. Relay ramp forms and normal fault linkages—Canyonlands National Park. Utah. Bulletin of the Geological Society of America 106, 1143–1157.

Walsh, J.J., Watterson, J., 1988. Analysis of the relationship between displacement and dimensions of faults. Journal of Structural Geology 10, 239–247.

Walsh, J., Watterson, J., Bailey, W., Childs, C., 1999. Fault relays, bends and branch-lines. Journal of Structural Geology 21, 1019–1026.

Walsh, J., Nicol, A., Childs, C., 2002. An alternative model for the growth of faults. Journal of Structural Geology 24, 1669–1675.

Walsh, J.J., Bailey, W.R., Childs, C., Nicol, A., Bonson, C.G., 2003. Formation of segmented normal faults: a 3-D perspective. Journal of Structural Geology 25, 1251–1262.

Willemse, E.J.M., 1997. Segmented normal faults: correspondence between three-dimensional mechanical models and field data. Journal of Geophysical Research 102, 675–692.

Willemse, E.J.M., Pollard, D.D., Aydin, A., 1996. Three-dimensional analyses of slip distributions on normal fault arrays with consequences for fault scaling. Journal of Structural Geology 18, 295–309.